Ultrasonics 65 (2016) 1–4

Contents lists available at ScienceDirect

Ultrasonics

journal homepage: www.elsevier.com/locate/ultras

Short Communication

Inverse characterization of plates using zero group velocity Lamb modes

Clemens Grünsteidl [a], Todd W. Murray [b], Thomas Berer [a], István A. Veres [a,*]

[a] Research Center for Non-Destructive Testing GmbH (RECENDT), Altenberger Str. 69, 4040 Linz, Austria
[b] Department of Mechanical Engineering, University of Colorado at Boulder, 427 UCB Engineering Center, Boulder, CO 80309, USA

ARTICLE INFO

Article history:
Received 15 August 2015
Received in revised form 12 October 2015
Accepted 14 October 2015
Available online 17 October 2015

Keywords:
Zero group velocity Lamb waves
Inverse problem
Laser-ultrasound

ABSTRACT

In the presented work, the characterization of plates using zero group velocity Lamb modes is discussed. First, analytical expressions are shown for the determination of the k–ω location of the zero group velocity Lamb modes as a function of the Poisson's ratio. The analytical expressions are solved numerically and an inverse problem is formulated to determine the unknown wave velocities in plates of known thickness. The analysis is applied to determine the elastic properties of tungsten and aluminum plates based on the experimentally measured frequency spectra.

1. Introduction

Zero group velocity (ZGV) points of the dispersion relations of plates provide a strong and easily detectable resonance-like frequency of the plate [1]. ZGV resonances can be excited with excellent efficiency using laser sources, making them attractive candidates for use in laser based ultrasonic inspection of plates [1–3]. To date, ZGV modes have been proposed for a wide range of applications including, for example, the determination of Poisson's ratio [4], measurement of the thickness and thickness profile of plates [5], characterization of cylindrical samples [6] and probing of interfacial stiffnesses between two plates [7].

Although ZGV frequencies possess high quality factors and provide exceptional sensitivity to material properties, their use in material characterization is less straightforward compared to conventional ultrasonic pulse-echo techniques [4]. This is primarily because their location in k–ω space is not easily accessible. Nevertheless, one can take advantage of the fact that Lamb wave dispersion curves can be normalized by the plate thickness and wave velocity, leaving the Poisson's ratio as the sole parameter governing the shape of the spectrum [8,9]. Measurement of two well-defined frequencies, such as the ZGV points, thus allows for the unique determination of Poisson's ratio in a plate with an unknown thickness [4].

In this paper, an analytical expression for the location of zero group velocity points is given and solutions for the lowest two zero group velocity points over a wide range of Poisson's ratio are provided. An inverse problem is formulated to evaluate the elastic properties of plates based on the measurement of two ZGV frequencies. The approach is demonstrated on aluminum and tungsten plates using experimentally measured spectra.

2. Location of the ZGV points

The Lamb wave spectra are found using the Rayleigh–Lamb frequency equations [10] for symmetric modes:

$$\Omega^s = \frac{\tan(hq)}{\tan(hp)} + \frac{4k^2pq}{(q^2-k^2)^2} = 0, \tag{1}$$

and for antisymmetric modes:

$$\Omega^a = \frac{\tan(hp)}{\tan(hq)} + \frac{4k^2pq}{(q^2-k^2)^2} = 0, \tag{2}$$

where

$$q = \sqrt{\left(\frac{\omega}{c_T}\right)^2 - k^2}, \quad p = \sqrt{\left(\frac{\omega}{c_L}\right)^2 - k^2}. \tag{3}$$

In Eqs. (1)–(3) $h = \frac{d}{2}$ denotes the half of the plate thickness d, ω is the angular frequency, c_L and c_T are the longitudinal and shear wave velocities, respectively, and k the wave number. A typical Lamb wave spectrum for a tungsten plate (with $\nu = 0.283$ and $c_T = 2673\ \mathrm{ms}^{-1}$) is plotted in Fig. 1(a). Two ZGV points are visible in the spectrum and are associated with the S_1 and A_2 modes. For metallic plates ($\nu \sim 0.30$) these are the only two ZGV modes that exist within the low frequency range shown on the figure. It has

* Corresponding author.
E-mail address: istvan.veres@recendt.at (I.A. Veres).

http://dx.doi.org/10.1016/j.ultras.2015.10.015
0041-624X/

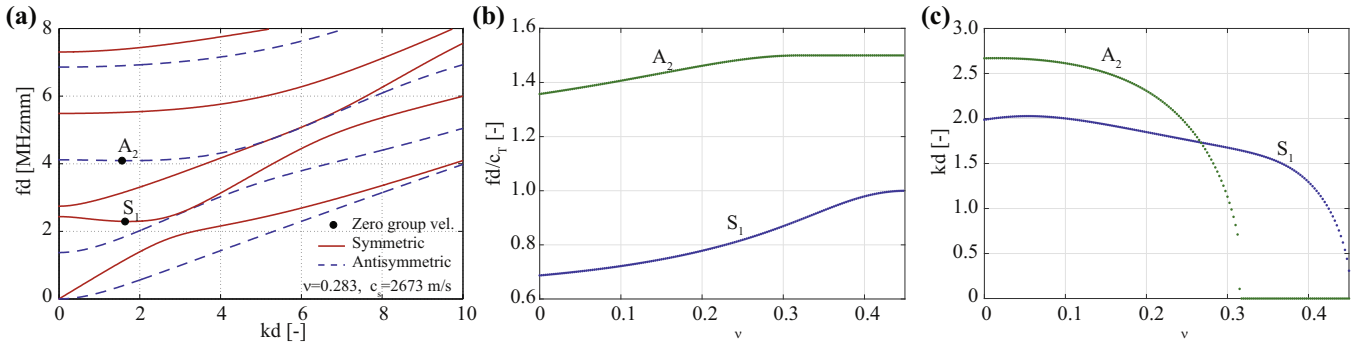

Fig. 1. (a) Dispersion relation of Lamb waves in a Tungsten plate with $\nu = 0.283$. ZGV points are visible for the S_1 and A_2 modes. (b) and (c) Location of the ZGV points in the $k-\omega$ plane for Poisson's ratios $0 < \nu < 0.45$.

been shown that these ZGV modes can be excited with high efficiency using a laser source [4,11,12].

For the practical use of the ZGV points, one must determine their location in the $k-\omega$ plane. ZGV points represent mathematically well-defined points within the dispersion relation as the wave number is nonzero and the group velocity vanishes. The latter is given through the implicit derivative for the symmetric modes as [10]:

$$c_G^s = \frac{d\omega}{dk} = -\frac{d\Omega^s}{dk}\left(\frac{d\Omega^s}{d\omega}\right)^{-1}, \tag{4}$$

or for antisymmetric modes as [10]:

$$c_G^a = \frac{d\omega}{dk} = -\frac{d\Omega^a}{dk}\left(\frac{d\Omega^a}{d\omega}\right)^{-1}. \tag{5}$$

The system of non-linear equations in Eqs. (1) and (4) or in Eqs. (2) and (5) describe the $k-\omega$ coordinates of the ZGV points in the case that $k \neq 0$ and cutoff frequencies if $k = 0$ [12]. The expressions for c_G^s and c_G^a are rather lengthy and they are given in Appendix A. The solution of the system of non-linear equations can be obtained numerically. Here, a Newton–Raphson iteration is used and the corresponding iteration process is given as:

$$\begin{bmatrix} k_{n+1} \\ \omega_{n+1} \end{bmatrix} = \begin{bmatrix} k_n \\ \omega_n \end{bmatrix} - \mathbf{J}^{-1} \begin{bmatrix} \Omega \\ c_G \end{bmatrix}. \tag{6}$$

where $\mathbf{J}$, Ω and c_G are evaluated at (k_n, ω_n). The Jacobian $\mathbf{J}$ is given as:

$$\mathbf{J} = \begin{bmatrix} \frac{\partial \Omega}{\partial k} & \frac{\partial \Omega}{\partial \omega} \\ \frac{\partial c_G}{\partial k} & \frac{\partial c_G}{\partial \omega} \end{bmatrix}, \tag{7}$$

where Ω and c_G must be replaced with Ω^s, c_G^s for the symmetric branches and with Ω^a, c_G^a for the antisymmetric branches. ZGV points and cutoff frequencies occur at multiple points in $k-\omega$ space, and thus the choice of the starting values for the wave number k and frequency f determines which points will be found. The derivation is carried out numerically. For the two lowest order modes of the symmetric and antisymmetric branches with ZGV points (S_1, A_2) the normalized $k-\omega$ coordinates of the ZGV points are plotted in Fig. 1(b) and (c) for a range of Poisson's ratios $(0 < \nu < 0.45)$. In agreement with previous findings, ZGV points exist only for a limited range of Poisson's ratios [4,11,13]. Otherwise, they degenerate to the cut-off frequencies of the mode and the wave vector vanishes. The cut-off frequency for the S_1 mode is given as [11,14]:

$$f = \frac{c_T}{d}, \ \left(\nu > \frac{1}{3}\right) \quad \text{and} \quad f = \frac{c_L}{2d}, \ \left(\nu \leqslant \frac{1}{3}\right). \tag{8}$$

For the A_2 mode, the cut-off frequency is given as:

$$f = \frac{3c_T}{2d}. \tag{9}$$

For the S_1 mode, the ZGV point exists for a wide range of isotropic materials having $\nu < 0.45$. However, for the A_2 mode its existence is limited to $\nu < 0.32$ [11]. Note that the cut-off frequency for the A_2 mode scales with $\frac{c_T}{d}$. Hence, for $\nu > 0.32$ the normalized frequency in Fig. 1(b) becomes constant and the wave vector goes to zero as shown in Fig. 1(c).

3. Solution approach

The Poisson's ratio of an isotropic plate can be determined with high accuracy by using two ZGV frequencies [4]. In addition, if the plate thickness is known then both elastic properties can be found. Although the basic idea is simple, the calculation of the locations of the ZGV points is more challenging. In Ref.[4], a set of curves were used to describe the ratios of the ZGV points. The curves were derived from the dispersion relation, calculated for a wide range of Poisson's ratios. Here, we present an alternative approach in which four non-linear equations (Eqs. (1)–(5)) are solved directly, yielding the unknown wave velocities c_L and c_T (or Poisson's ratio ν and one wave velocity c_T, for example). The wave numbers k_{ZGV}^s, k_{ZGV}^a, corresponding to the ZGV points, are also determined from this system, since the four equations allow for the evaluation of four unknowns. Again, the solution of the system of non-linear equations can be obtained numerically using a Newton–Raphson iteration:

$$\begin{bmatrix} \nu_{n+1} \\ c_{Tn+1} \\ k_{n+1}^s \\ k_{n+1}^a \end{bmatrix} = \begin{bmatrix} \nu_n \\ c_{Tn} \\ k_n^s \\ k_n^a \end{bmatrix} - \mathbf{J}^{-1} \begin{bmatrix} \Omega^s \\ c_G^s \\ \Omega^a \\ c_G^a \end{bmatrix}, \tag{10}$$

where Ω^s and c_G^s are evaluated at $(\nu_n, c_{Tn}, k_n^s, \omega_1)$ and Ω^a and c_G^a at $(\nu_n, c_{Tn}, k_n^a, \omega_2)$. The Jacobian in this case is given as:

$$\mathbf{J} = \begin{bmatrix} \frac{\partial \Omega^s}{\partial \nu} & \frac{\partial \Omega^s}{\partial c_T} & \frac{\partial \Omega^s}{\partial k} & 0 \\ \frac{\partial c_G^s}{\partial \nu} & \frac{\partial c_G^s}{\partial c_T} & \frac{\partial \Omega^s}{\partial k} & 0 \\ \frac{\partial \Omega^a}{\partial \nu} & \frac{\partial \Omega^a}{\partial c_T} & 0 & \frac{\partial \Omega^a}{\partial k} \\ \frac{\partial c_G^a}{\partial \nu} & \frac{\partial c_G^a}{\partial c_T} & 0 & \frac{\partial \Omega^a}{\partial k} \end{bmatrix}. \tag{11}$$

The Jacobian $\mathbf{J}$, is evaluated at $(\nu_n, c_{Tn}, k_n^s, \omega_1)$ for the symmetric mode and at $(\nu_n, c_{Tn}, k_n^a, \omega_2)$ for the antisymmetric mode, where ω_1, ω_2 denote the two experimentally measured ZGV frequencies. In practice, for most materials $(\nu < 0.45)$ the lower frequency ω_1

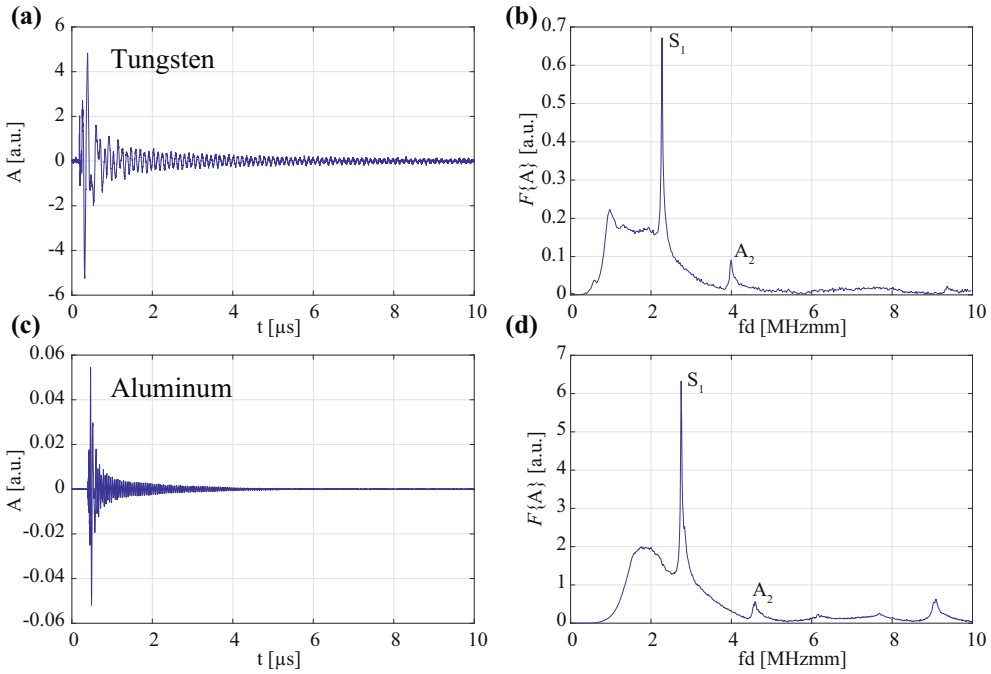

Fig. 2. Experimental signal and its Fourier transform for tungsten (a) and (b) and for aluminum (c) and (d) plates. The first two resonances indicated in the spectra are associated with symmetric and antisymmetric modes, respectively.

would correspond to the S_1 ZGV point and the upper frequency ω_2 would correspond to either the A_2 ZGV point ($\nu < 0.32$) or the A_2 cutoff frequency ($\nu > 0.32$). We note that in the numerical evaluation of these equations, care must be taken to avoid numerical instabilities in cases where the ZGV point degenerates to the cutoff frequency and k^a_{ZGV} goes to zero. The numerical approach requires starting values for the four unknowns, and suitable choices can be obtained by first estimating the Poisson's ratio and then using Fig. 1(b) and (c) as a guide to estimate the other unknowns. We give some examples of starting values in the following section.

4. Experimental results and analysis

The experimental setup is identical to the setup presented in Ref. [12]. A pulsed, frequency doubled Nd:YAG-laser (pulse energy ~ 10 μJ, pulse duration 500 ps, repetition rate 150 Hz) was focused onto the sample surface for ultrasound generation. The resulting surface displacement was detected on the opposite side of the sample with a stabilized Michelson interferometer. The interferometer output was recorded on an oscilloscope which was triggered by a photodiode sampling the excitation laser pulse. Low frequency oscillations associated with the A_0 Lamb mode were filtered out by a 1 MHz high-pass filter.

The inverse problem is demonstrated with a tungsten plate with 0.25 mm thickness and with an aluminum plate with a thickness of 0.125 mm. The recorded time domain signal for the first case is shown in Fig. 2(a) and the corresponding Fourier transform in Fig. 2(b). The broad background of the Fourier transforms is due to the low frequency oscillations during the first couple of μs in the time domain signals [12]. The two peaks at $f_1 d = 2.248$ MHz mm and $f_2 d = 3.997$ MHz mm correspond to the S_1 and A_2 ZGV points, respectively.

Using thickness-normalized values, the iteration was started at $\nu = 0.29$, $c_T = 2650\ \mathrm{ms}^{-1}$, $k^s_{ZGV} d = 1.70$, $k^a_{ZGV} d = 1.70$. The iteration process converged quickly (< 10 iterations) and the material properties were found as: $\nu = 0.272$, $c_T = 2678\ \mathrm{ms}^{-1}$. The wave numbers of the ZGV points, as additional outputs of the process, were found to be: $k^s_{ZGV} d = 1.725$, $k^a_{ZGV} d = 1.667$.

For aluminum, the Poisson's ratio is higher and the A_2 mode ZGV point could degenerate to the cut-off frequency of the mode with $k^a_{ZGV} = 0$. An aluminum plate with a thickness of 0.125 mm was evaluated. The recorded time domain signal is shown in Fig. 2(c) and the corresponding Fourier transform in Fig. 2(d). The two peaks at $f_1 d = 2.750$ MHz mm and $f_2 d = 4.587$ MHz mm correspond to the S_1 ZGV point and either the A_2 ZGV point or cutoff frequency (depending on the Poisson's ratio), respectively.

Again using thickness normalized values, the iteration was started at $\nu = 0.30$, $c_T = 2850\ \mathrm{ms}^{-1}$, $k^s_{ZGV} d = 1.70$, $k^a_{ZGV} d = 1.70$. The iteration process converged in < 10 iterations and the material properties were found as: $\nu = 0.326$, $c_T = 3058\ \mathrm{ms}^{-1}$. The wave numbers of the ZGV points, as additional outputs of the process, were found to be: $k^s_{ZGV} d = 1.625$, $k^a_{ZGV} d = 0$.

The material property estimates for aluminum and tungsten can be compared to the results of Clorennec et al. [4] who found $c_T = 3150\ \mathrm{ms}^{-1}$ and $\nu = 0.3383$ for Duralumin, and $c_T = 2963\ \mathrm{ms}^{-1}$ and $\nu = 0.2839$ for tungsten [4]. We note that while reasonable agreement is found, the properties are dependent on processing conditions and alloy content, which are not identical in the two cases and may explain the discrepancies in the reported values.

In conclusion, we have investigated the characterization of plates using two zero group velocity Lamb modes. We have derived analytical expression for the determination of the k—ω locations of ZGV points as a function of the material properties and solved the resulting non-linear equations using a Newton–Raphson technique. We have formulated an inverse problem to evaluate the elastic properties of plates based on the measurement of ZGV frequencies, and used the approach to determine the properties of aluminum and tungsten plates.

Acknowledgements

I.A. Veres and C. Grünsteidl acknowledge support from an ongoing research programs of the FWF Austrian Science Fund, Project

no. P 26162-N20; T.W. Murray gratefully acknowledges the support of this research by the National Science Foundation under Grant CMMI 1335426.

Appendix A. Analytical expressions for the group velocity

The group velocity of the Lamb waves is given through the implicit derivative of the Lamb wave spectrum shown in Eqs. (1) and (2). After some manipulations the group velocity of the symmetric modes is given as:

$$\begin{aligned} c_G = {} & [4k[q(-kp_{,k}(\tan p + p\sec^2 p) - 2p\tan p + q\tan q) - k^2\tan q] \\ & + q_{,k}(k^2 - q^2) \times [(q^2 + 2q\sin 2q - k^2)\sec^2 q \\ & - 4k^2 p\tan p]]/[4k^2 p_{,\omega} q(\tan p + p\sec^2 p) + q_{,\omega}[4k^2 p\tan p \\ & + (k^2 - q^2)[k^2 - q(q + 2\sin 2q)]\sec^2 q]] \end{aligned} \tag{A.1}$$

and for the antisymmetric modes:

$$\begin{aligned} c_G = {} & -[4k^3 p^2 q_{,k}(\tan q + q\sec^2 q) + p(k^2 - q^2) \\ & \times \sec^2 p[q^2(\sin 2p - kp_{,k}) - 2kqq_{,k}\sin 2p + k^2 \\ & \times (kp_{,k} + \sin 2p)] - kp_{,k}(k^2 - q^2)\tan p]/k[p(k^2 - q^2) \\ & \times \sec^2 p[p_{,\omega}(k^2 - q^2) - 2qq_{,\omega}\sin 2p] - p_{,\omega}(k^2 - q^2)^2 \\ & \times \tan p + 4k^2 p^2 q_{,\omega}(\tan q + q\sec^2 q)] \end{aligned} \tag{A.2}$$

where $p_{,\omega},\ q_{,\omega},\ p_{,k},\ q_{,k}$ are the partial derivatives of $p,\ q$ in Eq. (3).

References

[1] C. Prada, O. Balogun, T.W. Murray, Laser-based ultrasonic generation and detection of zero-group velocity Lamb waves in thin plates, Appl. Phys. Lett. 87 (19) (2005) 194109.
[2] D. Clorennec, C. Prada, D. Royer, T.W. Murray, Laser impulse generation and interferometer detection of zero group velocity Lamb mode resonance, Appl. Phys. Lett. 89 (2) (2006) 024101.
[3] I.A. Veres, T. Berer, C. Grünsteidl, P. Burgholzer, On the crossing points of the Lamb modes and the maxima and minima of displacements observed at the surface, Ultrasonics 54 (3) (2014) 759–762.
[4] D. Clorennec, C. Prada, D. Royer, Local and noncontact measurements of bulk acoustic wave velocities in thin isotropic plates and shells using zero group velocity Lamb modes, J. Appl. Phys. 101 (3) (2007) 034908.
[5] D. Clorennec, C. Prada, D. Royer, Laser ultrasonic inspection of plates using zero-group velocity Lamb modes, IEEE Trans. Ultrason. Ferroelectr. Freq. Control 57 (5) (2010) 1125–1132.
[6] M. Ces, D. Royer, C. Prada, Characterization of mechanical properties of a hollow cylinder with zero group velocity Lamb modes, J. Acoust. Soc. Am. 132 (1) (2012) 180–185.
[7] S. Mezil, J. Laurent, D. Royer, C. Prada, Non contact probing of interfacial stiffnesses between two plates by zero-group velocity Lamb modes, Appl. Phys. Lett. 105 (2) (2014) 021605.
[8] R. Mindlin, Mathematical theory of vibrations of elastic plates, in: 11th Annual Symposium on Frequency Control, 1957, pp. 1–40.
[9] J.D. Achenbach, Elsevier Science Publilsher, 1000 AE Amsterdam, The Netherlands, 1999, pp. 226–236
[10] J.L. Rose, Cambridge University Press, Cambridge, UK, 1999, pp. 137–142.
[11] C. Prada, D. Clorennec, D. Royer, Local vibration of an elastic plate and zero-group velocity Lamb modes, J. Acoust. Soc. Am. 124 (1) (2008) 203–212.
[12] C.M. Grünsteidl, T.W. Murray, I.A. Veres, Experimental and numerical study of the excitability of zero group velocity Lamb waves by laser-ultrasound, J. Acoust. Soc. Am. 138 (1) (2015) 242–250.
[13] K. Negishi, Existence of negative group velocities in Lamb waves, Jap. J. Appl. Phys. 26 (S1) (1987) 171–173.
[14] K. Graff, Wave Motion in Elastic Solids, Dover Publications Inc., Mineola, New York, 1991.